NASA Technical Memorandum 100998

NASA-TM-100998 19880017250

A Microcomputer Based Frequency-Domain Processor for Laser Doppler Anemometry

W. Clifton Horne and Desmond Adair

July 1988

NASA
National Aeronautics and
Space Administration

NASA Technical Memorandum 100998

A Microcomputer Based Frequency-Domain Processor for Laser Doppler Anemometry

W. Clifton Horne
Desmond Adair, Ames Research Center, Moffett Field, California

July 1988

National Aeronautics and
Space Administration

Ames Research Center
Moffett Field, California 94035

A Microcomputer Based Frequency-Domain Processor for Laser Doppler Anemometry

W. Clifton Horne*

Desmond Adair**

NASA Ames Research Center

Abstract

A prototype multi-channel laser Doppler anemometry (LDA) processor was assembled using a wide-band transient recorder and a microcomputer with an array processor for fast Fourier transform (FFT) computations. The prototype instrument was used to acquire, process, and record signals from a three-component wind tunnel LDA system subject to various conditions of noise and flow turbulence. The recorded data was used to evaluate the effectiveness of burst acceptance criteria, processing algorithms, and selection of processing parameters such as record length. The recorded signals were also used to obtain comparative estimates of signal-to-noise ratio between time-domain and frequency-domain signal detection schemes. These comparisons indicate that the FFT processing scheme allows accurate processing of signals for which the signal-to-noise ratio is 10 to 15 dB less than practical with counter processors.

Nomenclature

D	diameter of axisymmetric jet
f_L	filter passband low-frequency cutoff
f_H	filter passband high-frequency cutoff
f_0	center frequency of doppler burst
K	amplitude of signal
L	power spectral density of LDA signal
n	noise signal
N	noise aplitude factor
P_N	integrated noise power
P_S	integrated signal power
$(S/N)_F$	frequency-domain signal-to-noise ratio
$(S/N)_T$	time-domain signal-to-noise ratio
T	sampling window time interval
ρ	LDA burst time constant

I. Introduction

Laser Doppler anemometry (LDA) offers an indispensable method of obtaining nonintrusive, quantitative measurements of mean and turbulent velocity characteristics of a broad range of flows. An important measure of the performance of the optical and detection systems of the LDA is the signal-to-noise ratio (S/N) of the photodetector output. This signal must be analyzed to obtain an accurate estimate of the burst frequency. Time-domain LDA signal counter-processors provide accurate Doppler burst frequency measurements at high data rates when the S/N exceeds a threshold of approximately 10-15 dB. This S/N is often difficult to achieve with long focus, backscatter optical configurations, and other factors such as surface glare and seeding density variations (due to centrifugal flows, for example) compound the difficulty. Since the level associated with the white-noise component of the photo-detector increases with processor bandwidth, the S/N can be maximized by narrow-band filtering, but this may limit the velocity range and introduce biasing in flows with severe mean velocity gradients and turbulence intensities. Another problem associated with counter-processors is discretization or quantization error which masks turbulence intensities below about 0.5%, depending on the optical and electronic set-up.

Proposals for new processor designs which overcome the limitations of countertype processors have been recently made. Meyers[1] has proposed a frequency-domain processor which determines the burst frequency by interpolating the output of a bank of five digital filters. Meyers reports that the processor, which will sample at rates of up to 1 GHz, can process bursts with as few as 150 photons/burst and has a "residual" turbulence level of 0.2% for signals for which the burst frequency deviates from the mean by 20% or less.

It is also possible to digitize the signal at a high fixed rate and execute a discrete Fourier transform to determine the burst frequency. This approach has been applied by several groups,[2,3,4,5] and offers several benefits relative to counter-type processors which include insensitivity of S/N to processor bandwidth and greater noise immunity. Modarress and Tan[4] found that data acceptance rates using DFT processing improved by two orders of magnitude over counter processors. The method takes advantage of commercially available transient recorders with sampling rates of up to

*Aerospace Engineer.
**NRC Research Associate.

within the upper 40 dB of the 76 dB dynamic range. A block diagram of the instrumentation is shown in Fig. 2. The front-end detectors of the counter-processors were used to provide the logic signals required to initiate digitization of the signal.

IV. Processing Software

Test software included modules for acquisition, FFT card control, frequency data acceptance/rejection, and velocity component computation. A summary of module functions is included in the Appendix. In addition to programs for evaluating ensemble averages of the flow characteristics, test programs were written to evaluate burst S/N ratios for both time domain (counter-processor) and frequency-domain (FFT) processing, and to determine the effect of sample length on the accuracy of burst frequency measurement. This program was run with experimental data to evaluate the effectiveness of polynomial interpolation of the burst spectra to improve estimates of burst frequency.

A processing rate goal of 25 samples/sec was determined to be consistent with minimum wind tunnel sampling periods of 1 min, allowing 1500 samples/location. Initial versions of the program achieved five accepted sample pairs/sec. Current efforts to optimize the code are expected to achieve the sample rate goal without incorporating available hardware accelerators.

V. Results

Fast Fourier transform records for each burst, similar to Fig. 1b, were used to compare time-domain and frequency-domain detection schemes. A value for the time-domain S/N (as seen by the counter-processors) was estimated by calculating 10 times the common logarithm of the ratio of the sum of burst spectral components to the sum of the nonburst spectral components. The corresponding frequency-domain S/N value is 10 times the logarithm of the ratio of the peak burst spectral component to the peak nonburst component. This parameter characterizes the requirement of a software detector to extract the peak spectral component correctly from the array of spectral component values.

Figure 3 shows plots of frequency domain S/N v.s. time-domain S/N for two channels with differing noise levels. Typically, time-domain S/N values of 0 dB and 10 dB correspond to frequency-domain S/N values of 10 dB and 20 dB respectively. These values are somewhat lower than predicted in the previous analysis since the noise was integrated over the entire sample length, rather than the burst duration. For successful time-domain detection, a minimum detectable S/N value of 10-15 dB is required. For frequency-domain detection, a comparable difference between the peak burst level and the highest noise component is needed. This suggests that bursts can be correctly processed in the frequency domain which are 10-15 dB lower than accurately measurable with counter processors. Temporary storage of the digitized burst waveforms also permits more rigorous acceptance criteria than those employed with the counter processor, allowing greater confidence in the accepted data.

Fast Fourier transform computation time is proportional to N log(N), where N is the number of transform points. Efficient sorting and validation algorithms are comparably scaled. Thus higher throughput may be obtained at the expense of frequency resolution. The burst data was processed with FFT sizes of 1024, 512, 256, 128, 64, 32, and 16 points to determine the effect of record length on processor accuracy. In addition, the data was also processed after setting the first and last 25% of the samples of each burst record to zero, simulating the process of padding a shorter time series with zeros prior to executing the FFT.

The peak component of the FFT is an estimate of the actual frequency, which may be assumed to be uniformly distributed within an interval centered on the measured peak and equal to the frequency interval separating the components of the FFT. For this assumption, the standard deviation of the estimate is 0.289 times the frequency interval, a value which was confirmed by experiment. It is possible to improve this estimate by fitting a parabola to the three highest spectral levels, and then calculating the peak of the fitted parabola. The process is illustrated in Fig. 4, which shows the results of a 1024-point FFT and a 16-point FFT with a fitted parabola. In each case, the burst envelope was computed and the data was extracted from the burst center. The frequency error of reduced length estimates was taken as the difference between the reduced length estimate and the peak of the 1024-point FFT. The effect of sample size and S/N on this error is discussed below and in Figs. 5 and 6.

Figure 5 shows the locus of 50 sample pairs for the 32-sample FFT in coordinates of frequency-domain S/N and standard deviation of frequency estimate, in which the symbols 1 and 2 represent samples from the first and second velocity channels, respectively. The scatter of the samples in Fig. 5 suggests that frequency resolution is more dependent on record length than S/N for the selected sample population. A further examination of the results for the various record length FFTs showed that neither the simple peak-component estimate or the parabolic curve-fit estimate approached the high-resolution frequency estimate monotonically with record length, ruling out any successive approximation scheme. Other frequency estimation schemes, such as the maximum entropy method[9] may offer better results but were not considered in this study.

Figure 6 depicts the dependence of the standard deviation of reduced length estimates on record length. The three curves correspond to unpadded peak component estimates, and for parabolic interpolations of padded and unpadded records. As can be seen from Fig. 6, parabolic interpolation improves the resolution by 50%.* Replacing the first and last 25% of the data samples with zeros had no significant effect on the frequency estimate. This suggests that burst-length velocity biasing, as described in the background section, may be alleviated by zeroing a fixed number of samples outside the burst center without adversely affecting frequency resolution.

Velocity profiles of a 1.5-in.-diam axisymmetric jet with an nozzle speed of 32 m/sec were obtained to test the measurement and survey programs, and to detect serious biasing or defects in the hardware and software. A copy of a typical data sheet, with histograms for one location is presented in Fig. 7. Measurements of the mean velocity at a station four jet diameters downstream of the nozzle exit are presented in Fig. 8, with measurements from a hot-wire anemometer and LDA counter-processor for comparison. Similar comparisons of the normal and shear stresses for the axial and radial components are shown in Fig. 9. These results show generally good agreement between the two methods. Improved sampling rates will permit larger sample populations and greater confidence in the estimation and acceptance algorithms.

VI. Concluding Remarks

The present study demonstrated the feasibility of a microcomputer-based multichannel LDA signal processor using transient recorders and FFT. The throughput of this prototype processor is sufficient for most low-speed wind tunnel applications and the performance is superior to counter-processors for signals with S/N less than 10 dB. Preliminary evaluations of several processing algorithms were based on Doppler burst waveforms obtained from a multicomponent LDA. Results of these evaluations suggest that zeroing a fixed number waveform samples away from the burst center may minimize burst duration velocity biasing without adversely affecting frequency resolution, and that parabolic interpolation of the spectral components may improve the frequency resolution by about 50% relative to simply choosing the peak component. Continued trends of increasing computational and cost performance of microcomputer-based instrumentation should improve the availability of this approach as a cost-effective alternative to dedicated, nonprogrammable LDA signal processors.

References

1. Meyers, J. F.: Frequency domain laser velocimeter signal processor, 3rd International Symposium on Applications of Laser Anemometry to Fluid Mechanics, Lisbon, Portugal, July 7-9, 1986.

2. Pallek, D.: Fast digital data acquisition and analysis of LDA signals by means of a transient recorder and an array processor. ICASF Record, 1985, p. 309.

3. Layne, C.T, and Bomar, B.W.: Discrete Fourier transform laser velocimeter signal processor, ICIASF '87 Record, Williamsburg, VA, June 22-25, 1987, 87CG2449-7.

4. Modarress, D., and Tan, H.: A new digital signal processor for laser anemometry, International Specialists Meeting on the Use of Computers in Laser Velocimetry, St. Louis, France, May 18-20, 1987.

*This is consistent with the results by Durst et al. (Ref. 10).

5. Lading, L.: Spectrum analysis of LDA signals and postprocessing with a PC computer, International Specialists Meeting on the Use of Computers in Laser Velocimetry, St. Louis, France, May 18-20, 1987.

6. Durrani, T. S., and Greated, C. A.: Laser systems in flow measurement, Plenum Press, New York., 1977.

7. Orloff, K. L., Snyder, P.K., and Reinath, M. S.: Laser velocimetery in the low-speed wind tunnels at Ames Research Center, NASA TM 85885, Jan., 1984.

8. Adair, D., and Horne, W. C.: Turbulent separated flow in the vicinity of a single-slotted airfoil flap, AIAA 26th Aerospace Sciences Meeting, Reno, NV. Jan. 1988.

9. Lacoss, R. T.: Data adaptive spectral analysis methods, Geophysics, vol. 36, no. 4, August, 1971, pp. 661-675.

10. Durst, F., Howe, B., and Richter, G.: Long-range LDA wind velocity measurements using visible laser radiation, Proceedings of the 4th International Conference on Photon Correlation Techniques in Fluid Mechanics, Stanford University, California, August 25-27, 1980.

APPENDIX: SOFTWARE ORGANIZATION

(software modules in parenthesis)

A. Initialization

1. Initialize transient recorder and array processor (Set_up3, init_fftsys)
2. Input test parameters: digitizing rate, signal bandwidth mix frequency, number of samples acceptance criteria
3. Initialize graphics display (graph_init, text_init)

B. Acquisition Loop

1. Transfer data from transient recorder to computer upon receiving event pulse. (Trans2k)
2. Convert and scale data to 16-bit integer format (Trans2k)
3. Execute FFT and PSD (real_fft_psd)
4. Sort frequency data for largest element (sort1,sort2)
5. Accept/reject on basis of relative magnitude and location of next highest elements (reject if non-adjacent) (sort1,sort2)
6. Update statisitical quantities and graphics display (update)
7. Repeat for each channel until sample number requirement is fulfilled

C. Data processing/display

1. Compute turbulence quantities (avg)
2. Update graphical displays (print_avg)
3. Store data and move to next traverse location (copy)

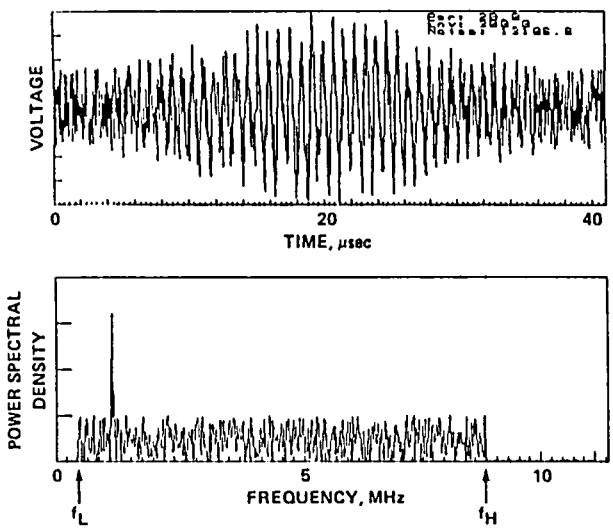

Figure 1. (1a) LDA single burst waveform. (1b) Single burst PSD.

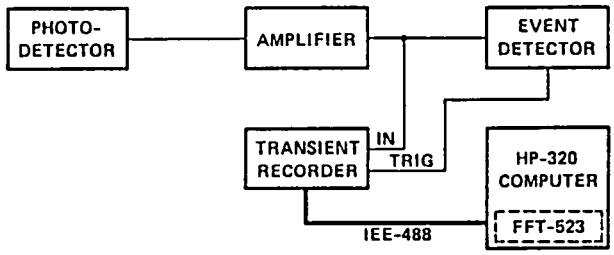

Figure 2. Instrumentation diagram (1 of 2 channels).

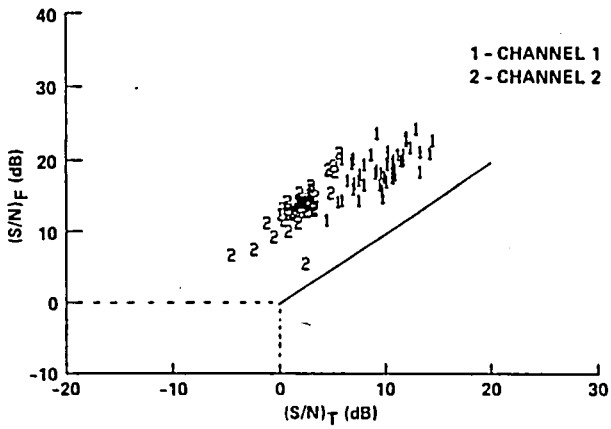

Figure 3. Typical variation of $(S/N)_F$ vs $(S/N)_T$.

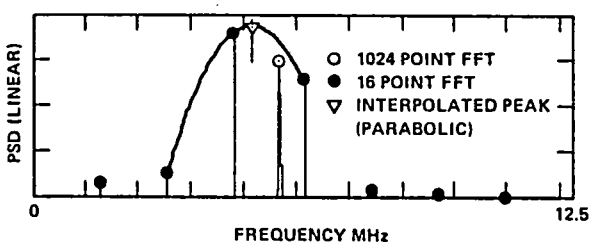

Figure 4. Parabolic interpolation of 16-point FFT and comparison with 1024-point FFT.

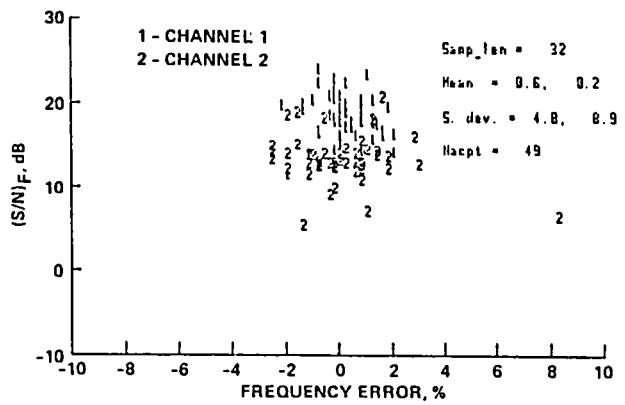

Figure 5. Typical distribution of interpolated frequency error.

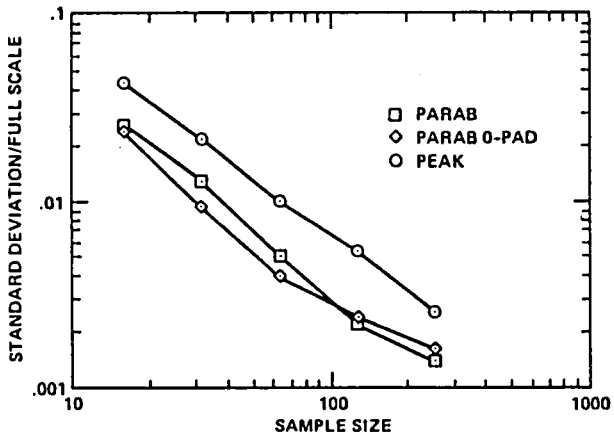

Figure 6. Effect of sample size on interpolated frequency error.

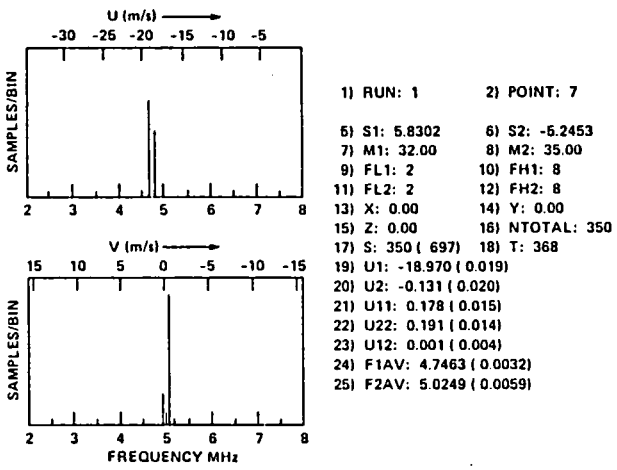

1) RUN: 1 2) POINT: 7

5) S1: 5.8302 6) S2: -5.2453
7) M1: 32.00 8) M2: 35.00
9) FL1: 2 10) FH1: 8
11) FL2: 2 12) FH2: 8
13) X: 0.00 14) Y: 0.00
15) Z: 0.00 16) NTOTAL: 350
17) S: 350 (697) 18) T: 368
19) U1: -18.970 (0.019)
20) U2: -0.131 (0.020)
21) U11: 0.178 (0.015)
22) U22: 0.191 (0.014)
23) U12: 0.001 (0.004)
24) F1AV: 4.7463 (0.0032)
25) F2AV: 5.0249 (0.0059)

Figure 7. Typical output page for two-channel set-up.

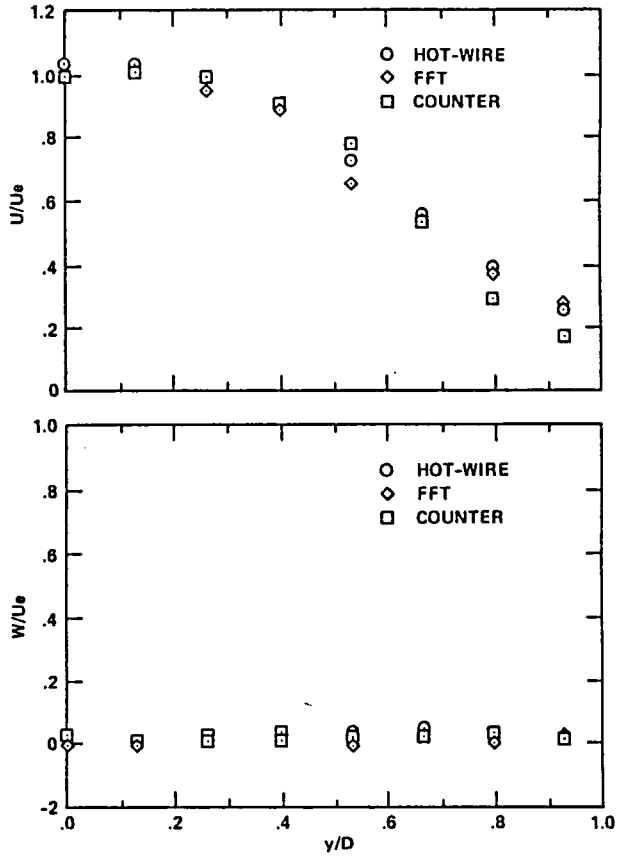

Figure 8. Mean velocity measurements of axisymmetric jet. Ue = 32 m/sec, D = 3.81 cm, x/D = 4.0.

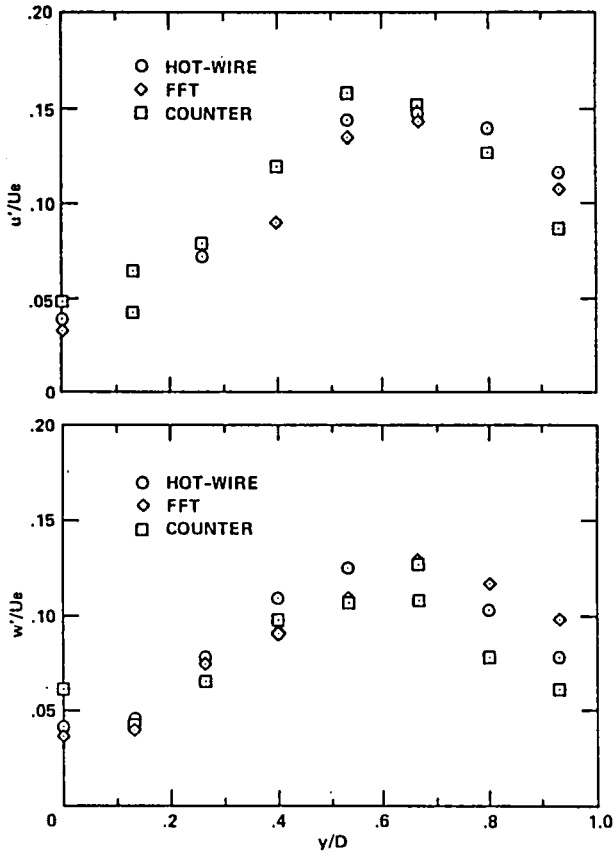

Figure 9. Turbulence measurements of axisymmetric jet. Ue = 32 m/sec, D = 3.81 cm, x/D = 4.0.

NASA
National Aeronautics and Space Administration

Report Documentation Page

1. Report No.	2. Government Accession No.	3. Recipient's Catalog No.
NASA TM 100998		

4. Title and Subtitle	5. Report Date
A Microcomputer Based Frequency-Domain Processor for Laser Doppler Anemometry	July 1988
	6. Performing Organization Code

7. Author(s)	8. Performing Organization Report No.
W. Clifton Horne and Desmond Adair	A 88173
	10. Work Unit No. 505-61-01

9. Performing Organization Name and Address	11. Contract or Grant No.
Ames Research Center Moffett Field, CA 94035	
	13. Type of Report and Period Covered
12. Sponsoring Agency Name and Address	Technical Memorandum
National Aeronautics and Space Administration Washington, DC 20546-0001	14. Sponsoring Agency Code

15. Supplementary Notes

Point of Contact: W. Clifton Horne, Ames Research Center, M/S 247-2
Moffett Field, CA 94035 (415) 694-6680 or FTS 464-6680

This paper was presented at the Fourth International Symposium on Applications of Laser Anemometry to Fluid Mechanics, July 11-14, 1988 in Lisbon, Portugal.

16. Abstract

A prototype multi-channel laser Doppler anemometry (LDA) processor was assembled using a wide-band transient recorder and a microcomputer with an array processor for fast Fourier transform (FFT) computations. The prototype instrument was used to acquire, process, and record signals from a three-component wind tunnel LDA system subject to various conditions of noise and flow turbulence. The recorded data was used to evaluate the effectiveness of burst acceptance criteria, processing algorithms, and selection of processing parameters such as record length. The recorded signals were also used to obtain comparative estimates of signal-to-noise ratio between time-domain and frequency-domain signal detection schemes. These comparisons indicate that the FFT processing scheme allows accurate processing of signals for which the signal-to-noise ratio is 10 to 15 dB less than is practical using counter processors.

17. Key Words (Suggested by Author(s))	18. Distribution Statement
Laser velocimetry Laser Doppler anemometry Fast Fourier transform	Unclassified-Unlimited Subject Category-34

19. Security Classif. (of this report)	20. Security Classif. (of this page)	21. No. of pages	22. Price
Unclassified	Unclassified	8	A02

NASA FORM 1626 OCT 86